Makara Journal of Science

Volume 21
Issue 1 *March*

Article 5

3-20-2017

Fe(III) Oxide-modified Indonesian Bentonite for Catalytic Photodegradation of Phenol in Water

Novia Arinda Pradisty
Department of Chemistry, Faculty of Mathematics and Natural Sciences, Universitas Indonesia, Depok 16424, Indonesia

Riwandi Sihombing
Department of Chemistry, Faculty of Mathematics and Natural Sciences, Universitas Indonesia, Depok 16424, Indonesia

Russell Francis Howe
Department of Chemistry, University of Aberdeen, Meston Building, Meston Walk, Aberdeen AB24 3UE, Scotland, United Kingdom

Yuni Krisyuningsih Krisnandi
Department of Chemistry, Faculty of Mathematics and Natural Sciences, Universitas Indonesia, Depok 16424, Indonesia, yuni.krisnandi@sci.ui.ac.id

Fe(III) Oxide-modified Indonesian Bentonite for Catalytic Photodegradation of Phenol in Water

Cover Page Footnote

The authors would like to thank Ms. Noer Fadlina Antra for the low-angle XRD measurement at the Department of Chemistry, University of Aberdeen. Part of this workwas also funded by TWAS Grant No. 13-034RG/CHE/AS_I-UNESCO FR: 3240277703.

Makara Journal of Science, 21/1 (2017), 25-33
doi: 10.7454/mss.v21i1.7534

Fe(III) Oxide-modified Indonesian Bentonite for Catalytic Photodegradation of Phenol in Water

Novia Arinda Pradisty[1], Riwandi Sihombing[1], Russell Francis Howe[2], and Yuni Krisyuningsih Krisnandi[1*]

1. Department of Chemistry, Faculty of Mathematics and Natural Sciences, Universitas Indonesia, Depok 16424, Indonesia
2. Department of Chemistry, University of Aberdeen, Meston Building, Meston Walk, Aberdeen AB24 3UE, Scotland, United Kingdom

[*]*E-mail : yuni.krisnandi@sci.ui.ac.id*

Received July 20, 2016 | Accepted December 1, 2016

Abstract

Phenol, which is a major organic pollutant, is usually detected in industrial wastewater, and thus the wastewater should be processed further before discharged into water bodies. Application of heterogeneous catalysis using natural-based materials is known to be effective and environmentally friendly in removing hazardous substances in water. In this study, local natural bentonite from the Tapanuli region in Indonesia was modified to eliminate dissolved phenol. Elimination by photodegradation reaction was conducted in a photo-Fenton system utilizing Fe(III) oxide-modified bentonite (Fe-B) as catalyst. Fe-B was prepared by a cation exchanging process using mixture solutions of NaOH and $FeCl_3$ with OH/Fe molar ratio of 2:1 and calcined at 300 °C. Material characterization was performed by X-ray diffraction (XRD), low-angle XRD, Fourier transform infrared spectroscopy and atomic absorption spectroscopy. The reaction components consisted of ultraviolet C light, H_2O_2, and Fe-B, and they were processed in a batch reactor. The role of each component was analyzed by a series of reaction conditions (i.e., adsorption, photolysis, H_2O_2 effect, Fenton, and homogeneous photo-Fenton). The heterogeneous photo-Fenton system was found to be essential for phenol degradation, as none of the reaction conditions caused total phenol removal in the 180 min reaction time. To conclude, heterogeneous photo-Fenton gave the highest photodegradation activity, and the best experimental condition for 1.10 mM phenol removal was 5 g L^{-1} catalyst, 78.35 mM H_2O_2, and 90 min reaction time.

Abstrak

Bentonit Indonesia Termodifikasi Fe(III) Oksida untuk Fotodegradasi Katalitik Fenol dalam Air. Fenol sebagai polutan organik utama sering terdeteksi dalam air limbah industri, sehingga air limbah tersebut perlu dilakukan pengolahan lebih lanjut sebelum dialirkan ke perairan. Aplikasi katalisis heterogen menggunakan material alamiah diketahui bersifat efektif dan ramah lingkungan untuk menghilangkan senyawa berbahaya di dalam air. Pada studi ini, bentonit alam lokal dari daerah Tapanuli di Indonesia dimodifikasi untuk mengeliminasi fenol terlarut. Eliminasi dengan reaksi fotodegradasi dilakukan menggunakan sistem foto-Fenton dengan bentonit termodifikasi Fe(III) oksida (Fe-B) sebagai katalis. Fe-B dipreparasi melalui proses pertukaran ion menggunakan larutan pemodifikasi yang terbuat dari NaOH dan $FeCl_3$ dengan rasio mol OH/Fe 2:1 dan dikalsinasi pada 300 ^oC. Karakterisasi material dilakukan dengan *X-ray diffraction* (XRD), *low-angle* XRD, *Fourier transform infrared spectroscopy* dan *atomic absorption spectroscopy*. Komponen reaksi yang tersusun oleh lampu ultraviolet C, H_2O_2, dan Fe-B diproses dalam reaktor *batch*. Peran dari setiap komponen dianalisis melalui serangkaian reaksi kontrol (adsorpsi, fotolisis, efek H_2O_2, Fenton dan foto-Fenton homogen). Sistem foto-Fenton heterogen terbukti memiliki peran penting dalam reaksi degradasi fenol, karena tidak satupun reaksi kontrol dapat menghilangkan fenol secara keseluruhan hingga waktu reaksi 180 menit. Kesimpulan yang didapatkan dari penelitian ini adalah reaksi foto-Fenton heterogen memberikan aktivitas fotodegradasi tertinggi dibandingkan reaksi lainnya dimana kondisi eksperimen terbaik untuk menghilangkan 1,10 mM fenol adalah 5 g L^{-1} katalis, 78,35 mM H_2O_2 dan waktu reaksi 90 menit.

Keywords: Fe-bentonite, photodegradation, photo-Fenton, phenol, water pollutant removal

Introduction

Industries are important pollution sources, and the discharged wastewaters may contain potentially harmful organic compounds. As a major organic pollutant, phenol is usually detected in various industrial wastewaters, namely, in petrochemical, tanneries, pulp and paper, chemical, and pharmaceutical industries [1]. As stated in

the Clean Water Act by the United States Environmental Protection Agency, phenol has been listed in the 126 priority pollutants since 1977 as one of the most hazardous water contaminants [2]. Nevertheless, water pollution from phenol and phenolic substances still remains high nowadays, especially in developing nations such as China, India, and Indonesia.

Phenol is harmful for both water organisms and human health [3]. Biodegradability of phenol is only 90% in surface water after seven days, and its aquatic toxicity (LC50) is 12 mg L^{-1} (*Daphnia magna*, 48 h). It is also classified in chronic health hazards as a teratogenic and carcinogenic agent [4-5]. For this reason, the maximum phenol concentration for safe consumption of drinking water is limited to 1 µg L^{-1} in Indonesia [6]. As phenol disposal into freshwater ecosystem without further treatment is dangerous for the environment, extensive research on phenolic wastewater treatment becomes exceptionally important.

The reaction of photo-Fenton has been highlighted as one of the most promising processes for wastewater treatments; reaction is classified as part of advanced oxidation processes [7]. The Fenton reagent consists of Fe catalyst and H_2O_2, and additional ultraviolet (UV) light radiation is added to trigger fast radical production [8-9]. The photo-Fenton reaction has two important steps: photoreduction of Fe^{3+} into Fe^{2+} and reoxidation of Fe^{2+} into Fe^{3+} by H_2O_2. The high reactivity of the resultant hydroxyl radical (OH) and hydroperoxyl radical (OOH) can oxidize and degrade organic pollutants into environmentally friendly products or even mineralize pollutants completely to produce CO_2 and H_2O [10-11]. The application of solid support to produce heterogeneous Fe catalyst in the photo-Fenton reaction can minimize the usage of Fe^{2+}/Fe^{3+}, thus resulting in high reproducibility and less additional Fe pollution after treatment [12].

The heterogeneous catalyst in the photo-Fenton reaction can be prepared by loading the active species to various materials, such as bentonite, sepiolite, hydrocalcite, zeolite, and mesoporous silica [13]. Bentonite has been proved to be one of the most promising support materials for catalyst because of its unique characteristics, great abundance, and cost efficiency [14]. In Indonesia, the abundance of natural bentonite as a mining resource is immense. Bentonite can be found in many places in Indonesia, especially in Sumatera, Java, Kalimantan, and Sulawesi. Unfortunately, the application of local bentonite in Indonesia is still limited compared with imported bentonite, with the national bentonite demand remaining at a ±20% deficit in 2010 [15].

Bentonite is produced by volcanic ash weathering and generally exists in form of Ca-bentonite (Ca-B), the cations of which can be exchanged to become Na-bentonite (Na-B). When Na-B comes in contact with water, it may swell several times from its initial volume. The main constituent mineral of bentonite is montmorillonite, a group of smectitic clay composed of repetitions of 2:1 clay layers. Each layer consists of one Al^{3+} octahedral sheet sandwiched between two Si^{4+} tetrahedral sheets [16]. The substitution of Al^{3+} or Fe^{3+} to Si^{4+} in the tetrahedral sheet and that of Mg^{2+}, Zn^{2+}, and Fe^{2+} to Al^{3+} in the octahedral sheet generate negative charges on the layer surfaces, which are neutralized by interlayer cations (e.g., K^+, Na^+, Ca^{2+}, or Mg^{2+}. The modification process, namely, ion exchange in the interlayer of montmorillonite can be established to modify bentonite as a heterogeneous catalyst [12].

The modification of bentonite as a heterogeneous catalyst for the photo-Fenton reaction can be made by the intercalation of Fe polycations using the cation exchange process and the resultant Fe–hydroxyl bentonite. By giving different treatments to Fe–bentonite, dissimilar kinds of Fe-modified bentonites can be produced. A comparative study by Chen and Zu (2009) [17] on the three types of Fe-modified bentonites, namely, Fe–hydroxyl-modified bentonite, α-Fe_2O_3-modified bentonite, and α-FeOOH-modified bentonite, concluded that Fe–hydroxyl-modified bentonite and α-Fe_2O_3-modified bentonite have a higher catalytic activity in the photo-Fenton system than the α-FeOOH-modified bentonite.

The aims of this study are (1) to prepare Fe(III) oxide-modified bentonite (Fe-B) from local natural bentonite using the cation exchange process, (2) to perform material characterization of the initial and modified bentonite, and (3) to assess the applicability of Fe-B as a heterogeneous catalyst for the photo-Fenton reaction to phenol removal in an aqueous solution. Before modifying the natural bentonite, pre-treatment, which involved the sedimentation and conversion from Ca-B to Na-B, was conducted to remove impurities and to create a desirable swelling bentonite. Material characterization for natural and modified bentonites was performed using X-ray diffraction (XRD), low-angle XRD, Fourier transform infrared (FTIR) spectroscopy, and atomic absorption spectroscopy (AAS). Phenol removal percentage at time intervals during reaction was recorded by an ultraviolet-visible (UV-vis) spectrophotometer. To ensure the effectiveness of Fe-B as a heterogeneous catalyst of a photo-Fenton reaction, seven related reaction conditions were also performed.

Experiment

Materials and chemicals. Indonesian natural Ca-B was gathered from Tapanuli, North Sumatera. NaCl, NaOH, HNO_3, HF, ethylenediamine, $CuSO_4.5H_2O$, H_2O_2 (30%), $FeCl_3.6H_2O$, and phenol were obtained from Merck and directly used without further purification.

Pre-treatment. Pre-treatment of Ca-B consisted of two subsequent steps, namely, sedimentation and Ca-B to Na-B

cation exchange process. Sedimentation was conducted by dispersing Ca-B into deionized water until 5 wt% Ca-B suspension was obtained and then stirred for 6 h. After stirring, the turbid suspension was carefully separated from solid impurities and kept overnight. Sediments in the turbid suspension (Ca-SB) were dried at 60 °C for two days and then grounded using mortar and pestle. The conversion of Ca-B into Na-B was conducted using the cation exchange process by adding 1 M NaCl into sedimented Ca-SB until the bentonite mass:NaCl volume ratio of 1:30 was exceeded and then stirred for 12 h. Afterward, Na-B was washed by deionized water in several runs until the concentration of chlorine ions in the filtrate decreased to 99% by a conductivity test. Na-B was dried at 105 °C for 3 h, grinded and sifted to obtain a bentonite particle size range of 315–100 µm. The cation exchange capacity (CEC) of Na-B was determined using the Cu-ethylenediamine complex absorption method initially published by Bergaya and Vayer (1997) [18-19]. The Cu-ethylenediamine complex before and after adsorption was determined by a double beam UV-vis spectrophotometer at λ_{max} = 548 nm. The result showed that CEC of Na-B was relatively small at 48.75 meq/100g.

Modification process. Fe (III) oxide-modified bentonites were prepared using the modified procedure from Tabet et al. (2006) [20]. First, a modifying solution was produced by adding 0.2 M $FeCl_3$ solution dropwise into a 0.4 M NaOH solution until an OH:Fe ratio 2:1 was produced. Aging in dark condition was applied to the modifying solution for eight days to form Fe polycations. After aging was completed, the intercalation of Fe–polycations into a bentonite interlayer was performed by adding the modifying solution stepwise into a 1 wt% colloidal aqueous suspension of Na-B and stirred vigorously at room temperature for 8 h. To remove excess Cl^-, the solids were separated immediately after stirring and then washed several times with deionized water by centrifugation. The resultant solids were dried at 105 °C, followed by grinding and sifting to produce Fe-B [105] with a particle size range of 300–105 µm. Finally, the modification process was performed by the mild calcination of Fe-B [105] at 300 °C for 3 h in a muffle furnace to finally produce Fe-B [300].

Material characterization. The XRD pattern measurement was taken on a Shimadzu XRD 7000 using Ni-filtered Cu Kα radiation (λ = 0.154 nm) as source (voltage 40 kV; current intensity 30 mA). Scan range of 2°–50° and scan rate of 2 (2θ)/min were applied for the measurement. The low-angle XRD patterns were measured by Bruker D8 Advance Powder Diffractometer with a scan range of 2°–15°. The FTIR spectra were recorded on a Shimadzu IR Prestige-21 spectrometer. The specimens were prepared by mixing the powder and KBr until the ratio of 1:10 was reached. The mixture was pressed into a pellet. An average of 100 scans was collected for each of measurement at a wavelength range of 300 cm^{-1}–4000 cm^{-1} and a resolution of 4 cm^{-1}.

Catalytic activity. To observe the catalytic activity of modified bentonites, the photocatalytic Fenton reaction to phenol was conducted inside a solarbox equipped with an ultraviolet C (UV-C) light (Phillips Unilux 15 W, λ_{max} = 245 nm) and a magnetic stirrer. In a typical procedure, a 50 mL beaker glass was filled with a mixture of 1.10 mM (100 ppm) phenol solution and 5 g L^{-1} catalyst stirred in dark condition for 1 min. The reaction began when the desired amount of H_2O_2 was added into the beaker and the UV-C lamp was turned on. Then, the reaction mixture was stirred for 180 min and sampling was performed for every 30 min. The UV-vis spectra of the sampling solutions were recorded on a Shimadzu UV-2450 spectrophotometer at a wavelength range of 200–400 nm. Through this result, phenol concentration was determined at λ_{max} = 269 nm, which was the characteristic absorption of phenol. The concentration was shown in the following phenol removal percentage:

$$\%\ Phenol\ removal\ = \frac{Co - Ct}{Co} \times 100\% \qquad (1)$$

In Eq. 1, C_t and C_o are the time-dependent concentration and initial concentration, respectively. H_2O_2 concentration was optimized by adding variations of 39.18, 78.35, 117.53, and 156.71 mM H_2O_2 solution into the reaction mixtures.

To ensure that the reaction occurred was based on Fenton photodegradation, seven related reaction conditions were also performed to compare the effect of different reactions

Table 1. Description of Reaction Conditions

Reaction condition	Reaction component					
	Phenol	UV	H_2O_2	0,2 M Fe^{3+}	Ca-B	Fe-B[300]
Adsorption by Ca-B	√	-	-	-	√	-
Adsorption by Fe-B[300]	√	-	-	-	-	√
H_2O_2 effect	√	√	-	-	-	√
Photolysis	√	√	-	-	-	-
Fenton by Fe-B[300]	√	-	√	-	-	√
Homogeneous photo-Fenton	√	√	√	√	-	-
Photo-Fenton by Ca-B	√	√	√	-	√	-
Photo-Fenton by Fe-B[300]	√	√	√	-	-	√

on phenol removal. The percentage of phenol removal was compared with the photo-Fenton reaction with Fe-B [300] (Table 1). The reaction conditions consisted of the adsorption process, photolysis, H_2O_2 effect, homogeneous Fenton, and heterogeneous photo-Fenton. The catalysts were differentiated using three kinds of catalysts: homogeneous 0, 2 M Fe^{3+}, and heterogeneous Ca-B and Fe-B [300]. The Fe percentages of Ca-SB and Fe-B [300] are determined by AAS (Shimadzu AA-6300) to determine the amount of Fe in both natural and modified bentonite and to investigate the probability of Fe leaching in the catalyst during the photo-Fenton reaction. Measurement of pH was also performed to determine the carboxylic acid formation.

Results and Discussion

XRD and low-angle XRD analysis. XRD patterns of Ca-B, Ca-SB, Na-B, Fe-B [105], and Fe-B [300] at 2θ = 2°–50° are shown in Figure 1 [A]. The occurrence of montmorillonite is determined by diffraction peaks at d_{001}, $d_{020-110}$, and d_{130}. The characteristic peaks of montmorillonite for Ca-B are found at 2θ = 5.53°, 19.98°, and 37.48°; Ca-SB at 2θ = 5.57°, 20.05°, and 37.52°; and Na-B at 2θ = 5.77°, 19.80°, and 37.70°. Nonclay components such as quartz and dolomite are also observed in the diffraction patterns. The characteristic diffraction peaks of quartz are exhibited at d_{100} and d_{101}, and those of dolomite are shown at d_{102} [21]. In these samples, the diffraction peaks of quartz and dolomite are found at 2θ = 20.84°, 26.60°, and 21.86° for Ca-B; 20.92°, 26.64°, and 21.91° for Ca-SB; and 2θ = 20.82°, 26.62°, and 21.86° for Na-B. From the comparison of d_{001} and nonclay intensities in Ca-B, Tapanuli natural bentonite contains a proportionate amount of montmorillonite, quartz, and dolomite.

Although the XRD patterns of Ca-SB and Ca-B are similar, the sedimentation process was found essential in removing visible bentonite impurities, such as amorphous carbon and calcite. Sharper diffraction peaks of montmorillonite, quartz, and dolomite in the Na-B diffraction pattern compared with Ca-B indicate that the sedimentation and cation exchange processes significantly increase the crystallinity of the bentonite structure. The higher d-spacing in Ca-B and Ca-SB (15.96 Å and 15.86 Å, respectively) than in Na-B (15.31 Å) may be explained by the presence of a calcium-rich sample, which is reduced after the preparation of Na-B (Figure 1 [B]) [22].

A small increment of d-spacing in Fe-B [105] compared with Na-B (15.31 Å) indicates the intercalation of small-sized Fe polycations into interlayer spaces of clay particles [27]. Yuan et al. (2008) [28] explained that the peak broadening at the d_{001} diffraction pattern in Fe-intercalated bentonite and Fe-pillared bentonite is due to the polymorphous size of intercalated Fe polycations. As the sizes of Fe polycations are not uniform, a heterogeneous intercalation occurs. Therefore, the different sizes of bentonite particles demonstrate dissimilar interlayer spaces, thereby giving a broad d_{001} diffraction.

In theory, the d-spacing of a pillared metal oxide bentonite should increase from its starting Na-B or Ca-B as a sign of metal polycation pillarization inside the bentonite interlayer spaces. However, in this experiment, the d-spacing of Fe-B [105] and Fe-B [300] does not significantly increase. The result shows that the stable Fe pillar structure from the hydrolysis of Fe salt is difficult to obtain, as Fe hydrated cations are likely to form discrete polyoxocation aggregates [29]. Therefore, a uniform pillar structure is not produced and adelaminated structure is

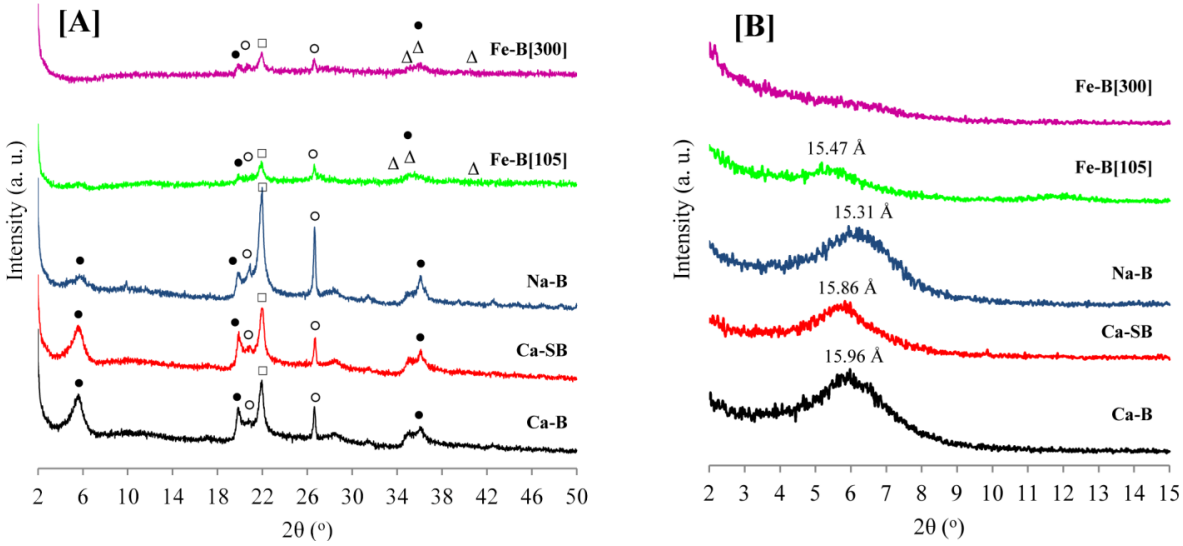

Figure 1. [A] X-ray and [B] low-angle X-ray Diffraction Pattern of Ca-B, Ca-SB, Na-B, Fe-B [105], and Fe-B [300]. Different Symbols in [A] are Used to Represent the Occurrence of Montmorillonite (●), Quartz (○), Dolomite (□), and Hematite/α-Fe_2O_3 (Δ), and the Numbers in [B] Indicate the d-spacing of Each Sample

produced instead. Moreover, a high concentration of Fe^{3+} in the pillaring solution compared with CEC of Na-B (133,33 meq 100 grams^{-1} vs. 48,75 meq 100 grams^{-1}) indicates a number of excess Fe polycations that cannot be intercalated into the bentonite interlayer spaces. Therefore, prepared Fe(III) oxide bentonite has the structure of Fe(III) oxide pillared-delaminated bentonite.

FTIR analysis. As shown in Figure 2, FTIR spectra of Ca-B, Ca-SB, and Na-B show similar vibration peaks. Every spectrum has a stretching characteristic vibration band from the hydroxyl groups (-OH) at 3629–3624 cm^{-1} from the stretching vibration of Al-Al-OH and Al-Mg-OH, which reflects the high amount of Al in montmorillonite octahedral sheets and the partial exchange of Mg with Al. A strong and broad absorption band at 3446–3421 cm^{-1} indicates absorbed water on bentonite surfaces reinforced by H-O-H deformation band of water at 1632–1620 cm^{-1}. Another absorption band at 1042–1038 cm^{-1} is due to the Si-O-Si vibration and that at 473–471 cm^{-1} is due to the Si-O bending and Fe-O stretching vibration. Impurities in bentonite are observed in the vibration band of Si-O quartz and silica at 798–796 cm^{-1} and in the stretching vibration band of silica overlapped by dolomite at 695–692 cm^{-1} [21,30]. In the Ca-SB and Na-B spectra, the weak vibration bands from quartz, silica, and dolomite suggest a decreasing amount of impurities after sedimentation.

Note that vibration bands from Fe generally overlap with the characteristic bands of montmorillonite; thus, the presence of Fe in bentonite is not resolved in the FTIR spectra, especially for the Fe-B [105] and Fe-B[300] spectra [28]. However, for both of the spectrum, low intensities are observed in the –OH bending vibration band from the structural hydroxyl groups in octahedral sheets at 3629 cm^{-1} and in the Si-O bending vibration band from tetrahedral sheets at 474 cm^{-1}. These observations may reflect the decreasing amount of free hydroxyl groups in the montmorillonite structure, and they support the XRD analysis than a high concentration of Fe was intercalated into the montmorillonite interlayer spaces.

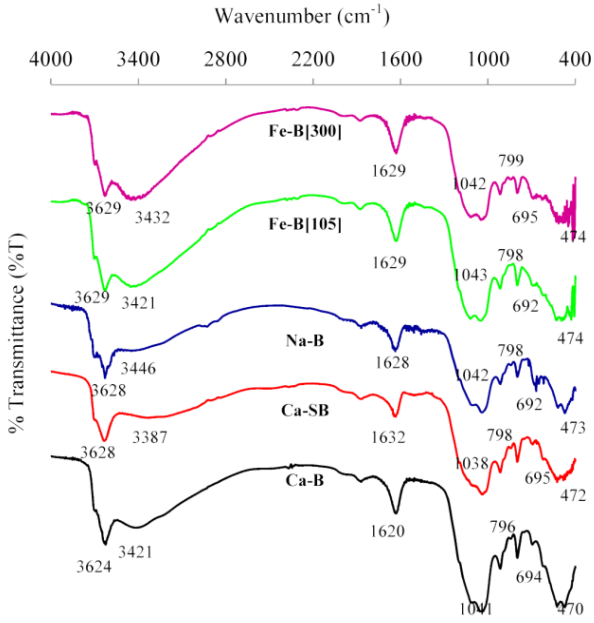

Figure 2. FTIR spectra of Ca-B, Ca-SB, Na-B, Fe-B [105], and Fe-B [300]

Catalytic activity. To assess the catalytic activity of Fe-B, a photo-Fenton reaction was performed to degrade phenol. UV-C light was used as the irradiation source because, unlike UV-A, it promotes two important reactions (i.e., photoreduction of Fe(III) into Fe(II) and direct decomposition of H_2O_2 to produce OH radicals [10]) in an organic compound degradation simultaneously. According to Iurascu et al. (2009) [31], the use of an irradiation source with a long wavelength, such as UV-A, only induces the photoreduction of Fe(III), thereby resulting in the decreased ability of system photo-degradation. For this reason, UV-C light was selected as the irradiation source for the photo-Fenton reaction in this experiment.

Based on the phenol calibration curve, the UV-vis spectra of phenol in various concentrations give two characteristic absorption peaks at 209 and 269 nm. Although the maximum absorption of phenol at 209 nm is higher than at 269 nm, absorbance at 209 nm is likely to shift at high concentrations. Therefore, the calibration curve of phenol is determined based on the maximum absorption at 269 nm. The existence of both absorption bands is associated with the $\pi \rightarrow \pi^*$ electronic transition from the aromatic ring of phenol [32]. When a photodegradation reaction occurs, the absorption bands decrease, thereby indicating the reduction of phenol concentration over the time. Partial phenol degradation produces diverse intermediates in the form of carboxylic acids, and total degradation produce CO_2 and H_2O as its complete mineralization products [14].

Determination of the optimum H_2O_2 concentration is important in the photo-Fenton reaction because every organic compound requires different H_2O_2 concentration. Previous researchers reported that the reaction occurs slower if the given H_2O_2 concentration is either too low or high [8]. A small concentration causes H_2O_2 to be insufficiently transformed into hydroxyl radical (HO·) and leads to a slow oxidation rate. By contrast, a high concentration induces the HO· scavenging reaction as follows:

$$H_2O_2 + HO\bullet \rightarrow HO_2\bullet + H_2O. \quad (2)$$

$$HO_2\bullet + HO\bullet \rightarrow H_2O + O_2 \quad (3)$$

Note that the hydroperoxyl radical (HO_2·) is less reactive than the hydroxyl radical (HO·)**.** Therefore, an increased H_2O_2 concentration shows a diminishing return in the reaction rate [33,34].

The photo-Fenton reaction to 1.10 mM phenol with four different H_2O_2 concentrations is shown in Figure 3. At a concentration of 39.18 mM, %phenol removal is only 60.43% after 180 min of reaction, thus indicating an inadequate H_2O_2 concentration given to the system. At a concentration of 78.35 mM, 100% phenol removal is achieved after 90 min.

At a concentration of 117.53 mM and 156.71 mM, %phenol removal is 98.82% and 37.27%, respectively, after 180 min. This result shows that the HO• radical scavenging reaction is likely to occur at a higher concentration (Eqs. (2) and (3)). With this optimization result, 78.35 mM H_2O_2 was used in the following photo-Fenton reaction to 1.10 mM phenol.

The photo-Fenton reaction has a number of reaction components. In this study, these reaction components are phenol as reactant, Fe-B [300] as a heterogeneous Fe catalyst, H_2O_2 as a strong oxidant, and UV-C light as an irradiation source. To determine the influence of each component, seven reaction conditions are performed for 180 min. The results are compared with those of the complete photo-Fenton reaction utilizing Fe-B [300]. The reaction condition comprises adsorption with Ca-SB and Fe-B [300], H_2O_2 effect, photolysis, homogeneous photo-Fenton, heterogeneous Fenton, and heterogeneous photo-Fenton with Ca-SB.

As shown in the reaction condition curve in Figure 4, the observation of phenol adsorption (non-catalytic reaction) using Ca-SB and Fe-B [300] after 180 min shows that phenol can be absorbed into bentonite by as much as 44.71% and 38.71%, respectively. In the H_2O_2 effect, which is the Fenton reaction without H_2O_2, only 29.98% of phenol is removed. This result shows that a strong oxidant has an important role in phenol photodegradation. Moreover, in photolysis, in which the phenol solution is irradiated only with UV-C light, the removal percentage is even lower than that in the H_2O_2 effect at only 12.35%. UV-C irradiation without the presence of H_2O_2 and either heterogeneous or homogeneous Fe catalyst cannot form HO•; thus, phenol degradation cannot be conducted effectively. A small percentage of phenol removal in the H_2O_2 effect and photolysis are assumed mainly from the adsorption process, not from the oxidation–photodegradation reaction, because it cannot produce radical species. In homogeneous photo-Fenton, where Fe^{3+} solution is added as the substitute for Fe-B [300] with the same Fe concentration, %phenol removal is even lower at only 2.67%. The low percentage is mainly caused by the increased turbidity of the reaction mixture after the addition of the Fe^{3+} solution, which acts as a coagulant. For this reason, only a small part of the emitted UV-C light is scattered, unable to be absorbed by the reaction mixture and eventually unable to induce a photo-Fenton reaction [31].

A better result is presented in the photo-Fenton reaction using Ca-SB, in which %phenol removal is found to be relatively high at 69.93% after 180 min. A photo-Fenton

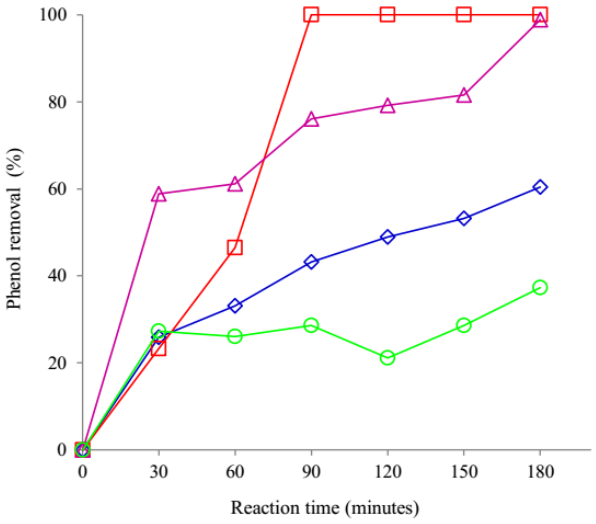

Figure 3. Comparison of Phenol Removal with Different Starting Concentrations of H_2O_2

[H_2O_2] : ◊ = 39.18 mM Δ = 117.53 mM
□ = 78.35 mM ○ = 156.71 mM
Initial condition: Fe-B [300] 5.0 g L^{-1}, [phenol] 1.10 mM, initial phenol pH 5.9

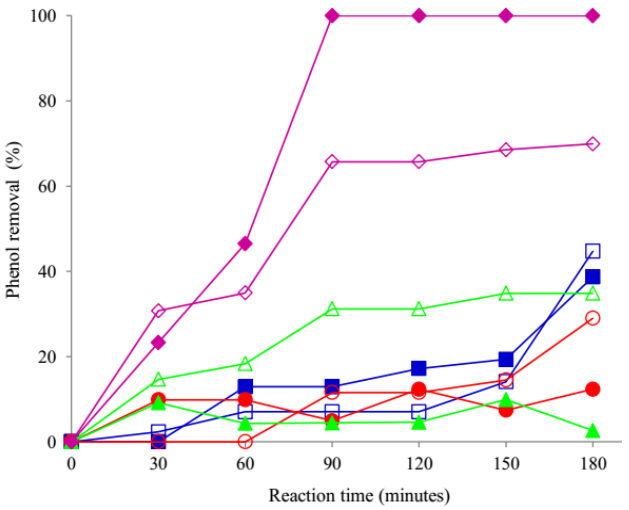

Figure 4. Phenol Removal Comparison of Eight Reaction Conditions

□ = Adsorption by Ca-SB
■ = Adsorption by Fe-B [300]
○ = H_2O_2 effect
● = Photolysis
△ = Het. Fenton by Fe-B [300]
▲ = Hom. photo-Fenton
◊ = Het. photo-Fenton by Ca-SB
♦ = Het. Photo-Fenton by Fe-B [300]
Initial condition: Ca-SB / Fe-B [300] 5.0 g L^{-1}, [phenol] 1.10 mM, $[H_2O_2]_{[B]}$ 78.35 mM, initial phenol pH 5.9

reaction may occur because Ca-SB naturally has a significant iron concentration (Table 2). Although Ca-SB can serve as a heterogeneous catalyst, note that in an aqueous solution, Ca-SB forms a colloidal suspension that is more difficult to separate than Fe-B [300], which has higher density. Photo-Fenton reaction using Fe-B [300] gives the highest %phenol removal that exceeds 100% after 90 min. Based on the comparison of reaction conditions, the photo-Fenton system using the Fe-B [300] catalyst is the most applicable system to degrade phenol in solution.

Post-reaction analysis. The stability of Fe-B [300] is reflected by its ability to maintain the Fe content in the bentonite structure during reaction. To determine Fe leaching during the photo-Fenton reaction, the percentage of Fe concentration in 100 g of bentonite (%Fe) is determined for Fe-B [300] before and after the photo-Fenton reaction. %Fe in Ca-SB is also determined to ascertain the Fe content in Tapanuli natural bentonite.

As shown in Table 2, significant Fe leaching is observed from the catalyst Fe-B [300] after 180 min of reaction. The presence of a low Fe concentration from catalyst leaching in the solution may contribute minimally to the catalysis in the photo-Fenton reaction by performing a homogeneous photocatalytic process with leached Fe^{3+} ions. However, the result also shows that the remaining %Fe in the Fe-B [300] catalyst after the reaction is 90.95%, which is still applicable if it is used for the subsequent photo-Fenton reaction. Consequently, Fe-B [300] is predicted to have good reusability properties, but re-calcination should be conducted first to eliminate the organic compounds trapped inside Fe-B [300].

The existence of acidic Fenton photodegradation products, which are carboxylic acids, is verified by pH observation before and after reaction. The results are presented in Table 3.

By comparing the initial and final solution pH for both of reactions, the solution pH decreased more in the photo-Fenton reaction than in the adsorption reaction, in which no photodegradation occurs. The higher ΔpH observed in the photo-Fenton reaction (2.88) than in the adsorption reaction (1.93) may have originated from the formation of carboxylic acids that have not completely

Table 2. %Fe in Ca-SB and Fe-B [300] Before and After the Photo-Fenton Reaction

Samples	% Fe 100 g^{-1} bentonite
Ca-SB	2.86
Fe-B [300] pre	8.77
Fe-B [300] post	7.98

Information:
Fe-B [300] pre: initial %Fe (t = 0 min)
Fe-B [300] post: final %Fe (t = 180 min)

Table 3. pH Changes During Photo-Fenton and Adsorption Reactions

Reaction	pH_{pre}	pH_{post}	ΔpH
Photo-Fenton	5.90	3.02	2.88
Adsorption	5.90	3.92	1.93

Information:
pH pre: initial solution pH (t = 0 min)
pH post: final solution pH (t = 180 min)
Δ pH: subtraction of pH pre–pH post

mineralized. Corresponding to Li *et al*. (2005) [35], the possible intermediates are muconic, maleic, succinic, malonic, oxalic, formic, and acetic acids in the photo-degradation of phenol or phenolic compounds in general. The complete mineralization of phenol produces H_2O and CO_2 as the end products. CO_2 is also considered to give acidic properties to the final solution because CO_2 is classified as a Lewis acid.

Conclusion

In this study, Fe-B is successfully prepared by the cation exchange process using natural Ca-B from Tapanuli, North Sumatera, Indonesia. The modifying solution with Fe^{3+} concentration exceeds the CEC and high OH to Fe molar ratio (2:1) results in Fe(III) oxide pillared-delaminated bentonite. This structure is proved by the Fe-B XRD pattern that demonstrates a smectite peak broadening at 2θ =2–8°.

The application of Fe-B as a heterogeneous catalyst in the Fenton photodegradation reaction with the addition of H_2O_2 as a strong oxidant can perform total phenol removal in the solution. The decrease in pH in the phenol solution after a photo-Fenton reaction indicates the existence of carboxylic acid intermediates that have not completely degraded. The assessment of reaction conditions indicates that each component in the hetero-geneous photo-Fenton system has an important role to perform for the effective phenol removal in the solution. We hope that our study findings will be applied as a promising alternative for industrial wastewater treatment in Indonesia.

Acknowledgements

The authors would like to thank Ms. Noer Fadlina Antra for the low-angle XRD measurement at the Department of Chemistry, University of Aberdeen. Part of this work was also funded by TWAS Grant No. 13-034 RG/CHE/AS_I- UNESCO FR: 3240277703.

References

[1] Dsikowitzky, L., Schwarzbauer, J. 2014. Industrial organic contaminants: identification, toxicity and

fate in the environment. J. Environ. Chem. Lett. 12(3): 371-386, doi: 10.1007/s10311-014-0467-1.
[2] United States Environmental Protection Agency (U.S. EPA). 2009. Human Health Criteria – Phenol, Retrieved from http://water.epa.gov/.
[3] Busca, G., Berardinelli, S., Resini, C., Arrighi, L. 2008. Technologies for the removal of phenol from fluid streams: A short review of recent developments. J. Hazard. Mater. 160 (2-3): 265-288, doi: 10.1016/ j.jhazmat.2008.03.045.
[4] Weber, M., Weber, M., Kleine-Boymann, M. 2008. Ullmann's Encyclopedia of Industrial Chemistry, John Wiley & Sons: New York.
[5] Hadjltaief, H.B., Costa P.D., Beaunier, P., Gálvez, M.E., Zina, M.B. 2014. Fe-clay-plate as a heterogeneous catalyst in photo-Fenton oxidation of phenol as probe molecule for water treatment. Appl. Clay Sci. 91-92: 46-54, doi: 10.1016/j.clay. 2014.01.020.
[6] Lampiran Peraturan Pemerintah Republik Indonesia No. 82 Tahun 2001, PPRI, Jakarta, p.2. [In Indonesian].
[7] Herney-Ramirez, J., Vicente, M., Madeirac, L. (2010). Heterogeneous photo-Fenton oxidation with pillared clay-based catalysts for wastewater treatment: A review. Appl. Catal. B. 98: 10-26, doi: 10.1016/j.apcatb.2010.05.004.
[8] Buxton, G.V., Greenstock, C.L. 1988. Critical Review of rate constants for reactions of hydrated electrons, hydrogen atoms and hydroxyl radicals (OH/O− in Aqueous Solution. J. Phys. Chem. Ref. Data 17(2): 513-886, doi: 10.1063/1.555805.
[9] Sum, O., Feng, J., Hu, X., Yue, P. 2005. Photo-assisted Fenton mineralization of an azo-dye Acid Black 1 using a modified laponite clay-based Fe nanocomposite as a heterogeneous catalyst. Top. Catal. 33: 233-242, doi: 10.1007/s11244-005-2532-2.
[10] Neyens, E., Baeyens, J. 2003. A review of classic Fenton's peroxidation as an advanced oxidation technique. J. Hazard. Mater. 98(1-3): 33-50. doi: 10.1016/S0304-3894(02)00282-0.
[11] Bautista, P., Mohedano, A.F., Casas, J.A., Zazo, J.A., Rodriguez, J.J. 2008. An overview of the application of Fenton oxidation to industrial wastewaters treatment. J. Chem. Technol. Biotechnol. 83: 1323-1338. doi: 10.1002/jctb.1988.
[12] Navalon, S., Alvaro, M., Garcia, H. 2010. Heterogeneous Fenton catalysts based on clays, silicas and zeolites. Appl. Catal. B. 99(1-2): 1-26. doi: 10.1016/j.apcatb.2010.07.006.
[13] Bergaya, F.A. 2008. Layered clay minerals: Basic research and innovative composite applications. Micropor. Mesopor. Mater. 107(1): 141-148. doi: 10.1016/j.micromeso.2007.05.064.
[14] Serwicka, E.M., Bahranowski, K. 2004. Environmental catalysis by tailored materials derived from layered minerals. Catal. Today 90(1-2): 85-92, doi: 10.1016/j.cattod.2004.04.012.
[15] Panjaitan. R.R. 2010. Kajian penggunaan bentonit dalam industri. Berita Litbang Industri XLV(3): 22-28. [In Indonesian].
[16] Chen, J., Zu, L. 2009. Comparative study of catalytic activity of different Fe-pillared bentonites in the presence of UV light and H_2O_2. Sep. Purif. Technol. 67(3): 282-288, doi: 10.1016/j.seppur. 2009.03.036.
[17] Bergaya, F., Vayer, M. 1997. CEC of clays: Measurement by adsorption of a copper ethylenediamine complex. Appl. Clay Sci. 12(3): 275-280, doi: 10.1016/S0169-1317(97)00012-4.
[18] Bergaya, F., Lagaly, G., Vayer, M. 2006. Cation and anion exchange. In F. Bergaya, B. Theng, & G. Lagaly, Handbook of clay science (pp. 979 – 995). Netherlands: Elsevier Ltd.
[19] Tabet, D., Saidi, M., Houaria, M., Pichat, P., Khalaf, H. 2006. Fe-pillared clay as a Fenton-type heterogeneous catalyst for cinnamic acid degradation. J. Environ. Manage. 80(4): 342-346, doi: 10.1016/j.jenvman.2005.10.003.
[20] Caglar, B., Afsin, B., Eren, E. 2009. Characterization of the cation-exchanged bentonites by XPRD, ATR, DTA/TG analyses and BET measurement. Chem. Eng. J. 149: 242-248, doi: 10.1016/j.cej.2008.10.028.
[21] Chipera, S.J., Bish, D.L. 2001. Baseline studies of the clay minerals society source clays: powder X-ray diffraction analyses. Clays Clay Miner. 49(5): 398-409, doi: 10.1346/CCMN.2001.0490507.
[22] Ayodele, O.B., Hameed, B.H. 2013. Synthesis of copper pillared bentonite ferrioxalate catalyst for degradation of 4-nitrophenol in visible light assisted Fenton process. J. Ind. Eng. Chem. 19(3): 966-974, doi: 10.1016/j.jiec.2012.11.018.
[23] Carriazo, J.G. 2012. Influence of iron removal on the synthesis of pillared clays: A surface study by nitrogen adsorption, XRD and EPR. Appl. Clay Sci. 67-68: 99-105, doi: 10.1016/j.clay.2012.07.010.
[24] Nogueira, F.G.E., Lopes, J.H., Silva, A.C., Lago, R.M., Fabris, J.D., Oliveira, L.C.A. 2011. Catalysts based on clay and iron oxide for oxidation of toluene. Appl. Clay Sci. 51(3): 385-389, doi: 10.1016/j.clay.2010.12.007.
[25] Deng, M.C., Chen, L.H., Hung, M.P., Chin, T.S., Lin, C.H. 1989. Preparation of gamma iron oxide particulate by a low temperature flux method. IEEE Trans. Magn. 25(5): 3644-3646, doi: 10.1109/20. 42387.
[26] Yuan, P., He, H., Bergaya, F., Wu, D., Zhou, Q., Zhu, J. 2006. Synthesis and characterization of delaminated iron-pillared clay with meso-microporous structure. Micropor. Mesopor. Mater. 88: 8-15, doi: 10.1016/j.micromeso.2005.08.022.
[27] Yuan, P., Bergaya, F.A., Tao, Q., Fan, M., Liu, Z., Zhu, J., He, H., Chen, T. 2008. A combined study by XRD, FTIR, TG and HRTEM on the structure of delaminated Fe-intercalated/pillared clay. J.

Colloid Interface Sci. 324(1-2): 142-149, doi: 10.1016/j.jcis.2008.04.076.

[28] Jolivet, J.P., Tronc, E., Chanéac, C. 2006. Iron oxides: From molecular clusters to solid. A nice example of chemical versatility. C. R. Geosci. 338: 488-497, doi: 10.1016/j.crte.2006.04.014.

[29] Daud, N., Ahmad, M., Hameed, B. 2010. Decoloriza-tion of Acid Red 1 dye solution by Fenton-like process using Fe–Montmorillonite K10 catalyst. Chem. Eng. J. 165: 111-116, doi: 10.1016/ j.cej.2010.08.072.

[30] Iurascu, B., Siminiceau, I., Vione, D., Vicente, M., Gil, A. 2009. Phenol degradation in water through a heterogeneous photo-Fenton process catalyzed by Fe-treated laponite. Water Res. 43(5): 1313-1322, doi: 10.1016/j.watres.2008.12.032.

[31] Duan, X., Ma, F., Yuan, Z., Chang, L., Jin, X. 2012. Electrochemical degradation of phenol in aqueous solution using PbO_2 anode. J. Taiwan Inst. Chem. E. 44: 95-102, doi: 10.1016/j.cej.2010.08.072.

[32] Chen, Q., Wu, P., Li, Y., Zhu, N., Dang, Z. 2009. Heterogeneous photo-Fenton photodegradation of reactive brilliant orange X-GN over iron-pillared montmorillonite under visible irradiation. J. Hazard. Mater. 168: 901-908, doi: 10.1016/j.jhazmat.2009. 02.107.

[33] Najjar, W., Azabou, S., Sayadi, S., Ghorbel, A. 2007. Catalytic wet peroxide photo-oxidation of phenolic olive oil mill wastewater contaminants: Part I. Reactivity of tyrosol over (Al–Fe)PILC. Appl. Catal. B: Environ. 74(1-2): 11-18, doi: 10.1016/j.apcatb.2007.01.007.

[34] Li, X.Y., Cui, Y.H., Feng, Y.J., Xie, Z.M., Gu, J.D. 2005. Reaction pathways and mechanisms of the electrochemical degradation of phenol on different electrodes. Water Res. 39(10): 1972-1981, doi: 10.1016/j.watres.2005.02.021.